Comparative study of three probabilistic methods for seismic hazard analysis: Case studies of Sochi and Kamchatka

V. A. Pavlenko · A. Kijko

Abstract This study examines the effect of the procedures used in three different probabilistic seismic hazard analysis (PSHA) methods for estimating the rates of exceedance of ground motion. To evaluate the effect of these procedures, the Cornell-McGuire and Parametric-Historic methods, and the method based on Monte Carlo simulations are employed, and the seismic source model, based on spatially smoothed seismicity, is used in the calculations. Two regions in Russia were selected for comparison, and seismic hazard maps were prepared for return periods of 475 and 2475 years. The results indicate that the choice of a particular method for conducting PSHA has relatively little effect on the hazard estimates. The Cornell-McGuire method yielded the highest estimates, with the two other methods producing slightly lower estimates. The variation among the results based on the three methods appeared to be virtually independent of the return period. The variation in the results for the Sochi region was within 6%, and that for the Kamchatka region was within 10%. Accordingly, the considered PSHA methods would provide closely related results for areas of moderate seismic activity; however, the difference among the results would apparently increase with increasing seismic activity.

Keywords Probabilistic seismic hazard analysis · The Cornell-McGuire method · The Parametric-Historic method · Monte Carlo simulations

1 Introduction

The probabilistic seismic hazard analysis (PSHA) methodology allows estimation of the probability that various ground motion levels would be exceeded at a particular site during a specified time interval. Such analysis should precede the construction of infrastructure facilities in seismically active regions. At present, the Cornell-McGuire method (Cornell, 1968; McGuire, 1976; 1978) is applied most frequently for PSHA. This method incorporates information on seismic source zones (in the form of active faults or areal sources), frequency-magnitude distributions (e.g. the Gutenberg-Richter relation), and ground motion prediction equations (GMPEs) to estimate seismic hazard at a particular site. In this method, considerable attention is paid to the problem of accounting for various uncertainties (Budnitz et al., 1997), by using probability distributions (aleatory variability) and logic trees (epistemic uncertainties).

V. A. Pavlenko · A.Kijko
University of Pretoria Natural Hazard Centre, Pretoria, South Africa
E-mail: pavlenko.vasily@gmail.com, andrzej.kijko@up.ac.za

The initial step of the Cornell-McGuire method requires delineating the seismic sources, which are characterised by uniform spatial distribution of seismicity and homogeneous seismic parameters. Over time, it has become clear that the uniform distribution in many instances does not reflect the actual spatial distribution of epicentres (e.g. Wiemer et al., 2009; Spada et al., 2011). Moreover, the process of defining the source zones can be difficult and subjective, potentially leading to significant differences in the resulting source geometries prepared by different groups of experts (e.g. McGuire, 1993; Frankel, 1995; Budnitz et al., 1997). In addition, the estimation of the seismic parameters in areas of relatively low seismicity presents a substantial problem.

Such difficulties have stimulated the development of alternative methods that do not require the definition of the seismic source zones. These methods include, e.g. the techniques of Milne and Davenport (1969) and Veneziano et al. (1984) that are based entirely on the information from the seismic event catalogues, the methods of Frankel (1995) and Woo (1996) that use the spatial smoothing of seismicity, and the method of Kijko and Graham (1998; 1999) that combines the strong features of the previous techniques. In addition, there are PSHA procedures based on the Monte Carlo simulations (e.g. Ebel and Kafka, 1999; Musson, 2000; Shumilina et al., 2000; Assatourians and Atkinson, 2013).

In view of these different PSHA methods, the question is how the hazard estimates resulting from these different methods corresponded. In large countries, such as Russia, where seismogenic provinces differ significantly, different groups of experts often use different methods to analyse the seismic hazard in their regions (e.g. Shumilina et al., 2000; Yemanov et al., 2007). In such instances, it is important to know in what way the results of these analyses corresponded to each other.

Several studies have been devoted to this question, such as those by Molina et al. (2001), Beauval et al. (2006), Hong et al. (2006), and Goda et al. (2013). These studies were primarily focused on investigating the influences of different seismicity models on the estimated seismic hazard.

Molina et al. (2001) and Beauval et al. (2006) have compared the hazard estimates obtained with the conventional zoning approach - the basis of the Cornell-McGuire method - with those obtained by using the Kernel Smoothing method of Woo (1996). Using synthetic earthquake catalogues, Hong et al. (2006) conducted a comparison of seismic hazard estimates based on the Cornell-McGuire method, the Davenport-Milne method, and the Epicentral Cell method (an extension of the latter). Goda et al. (2013) used synthetic earthquake data to evaluate the effects of different smoothing approaches by employing the Cornell-McGuire, the Kernel Smoothing, and the Epicentral Cell methods.

The findings of these studies have demonstrated, among other things, that the assumption of a homogeneous activity rate within a seismic source zone is a poor representation of the true activity rate (Molina et al., 2001). In addition, it was shown that the hazard estimates based on the conventional zoning approach are generally higher than are those based on other approaches to seismic source modelling.

In addition to the differences of the applied seismic source models, the existing PSHA methods use different procedures to estimate the rates of exceedance of ground motion. In contrast with previous comparative studies, the current work is focused on investigating the effect of the procedures used in the different PSHA methods to estimate the exceedance rates. Based on the same seismic source model, three major PSHA methodologies are compared, namely, the conventional Cornell-McGuire method, the Parametric-Historic method, and the method based on Monte Carlo simulations.

2 Materials and Methods

2.1 Earthquake catalogue

The main earthquake catalogue used in this study represents the entire territory of Eurasia, and the timespan is from ancient times to the end of 2011. These data were generously provided by Dr Nina Medvedeva from the Schmidt Institute of Physics of the Earth of the Russian Academy of Sciences (http://ifz.ru). During the preparation of the catalogue, all dependent seismic events were removed by using the declustering

algorithm of Gardner and Knopoff (1974). The catalogue lists the date, epicentral coordinates, focal depth, and the surface-wave magnitude M_s of each event, and, for some events, the focal intensity and the azimuth of rupture propagation are available.

Two areas in Russia have been selected for investigation in this study, namely, the city of Sochi on the Black Sea coast and surrounding area, and the Kamchatka Peninsula in far eastern Russia. Both these areas are characterised by high seismic activity, with the seismicity of Sochi and surroundings being characterised by crustal earthquakes and that of Kamchatka by subduction earthquakes. Moreover, the characteristics of the radiation and propagation of seismic waves in these two areas differ substantially (Pavlenko, 2011).

More recent (2012-2016) seismic data for the selected areas were obtained from the United States Geological Survey (USGS) website (http://earthquake.usgs.gov/earthquakes/search/). The USGS data mostly provide the body-wave magnitude m_b. The same declustering algorithm (Gardner and Knopoff, 1974) was applied to these data to remove clusters and dependent seismic events. To obtain a homogeneous catalogue, magnitudes were converted to the moment magnitude scale M_w. Conversions were performed, based on the regional relations, if available; otherwise, global relations were applied. Therefore, small values of m_b in the regional catalogue for the Sochi area were converted by using the relation of Gasperini et al. (2013), which is based on the European-Mediterranean dataset. Conversions of both m_b and M_s for the Kamchatka Peninsula were performed by using the regional relations obtained by Gusev (1991); outside of the applicability ranges of regional relations, global relations were used. The adopted conversion scheme is shown in Table 1.

The resulting catalogue for the Sochi area contains 3958 earthquakes, with M_w from 3.0 to 8.1; whereas, that for the Kamchatka Peninsula contains 10389 earthquakes, with M_w from 3.6 to 9.0. The epicentres of these earthquakes are shown in Figs. 1 and 2. By using the cumulative plots of the number of seismic events as a function of time, the regional catalogues have been divided into sections, i.e. those containing pre-instrumental historical records and those containing complete instrumental earthquake data. For each instrumental sub-catalogue, the magnitude of completeness M_c was estimated based on the procedure proposed by Amorèse (2007).

2.2 Seismic source model

The seismic source model used in this study resembles the approach proposed by Frankel (1995) for mapping seismic hazard in the United States (e.g. Frankel et al., 2002; Petersen et al., 2014). The area of study is covered by a regular grid of points forming a square of cells. Each cell is treated as a point seismic source and earthquakes are assumed to occur as a stationary Poisson process with constant rate Λ.

The frequency-magnitude distribution (FMD) describes the relation between the frequency of occurrence and the magnitude of earthquakes. The most common FMD in seismic hazard studies is the Gutenberg-Richter relation (Gutenberg and Richter, 1944):

$$\log_{10} N(M) = a - bM \tag{1}$$

where $N(M)$ is the number of seismic events with magnitude equal to or greater than M, a is a measure of the level of seismic activity, and b is the slope of the recurrence curve.

If the magnitudes of the seismic events are assumed to be independent identically distributed random variables, and the magnitude range is bounded from the top, then, the distribution of magnitude has the form of a truncated exponential distribution, with the following cumulative distribution function (CDF):

$$F_M(m) = \frac{1 - \exp\left[-\beta(m - M_c)\right]}{1 - \exp\left[-\beta(M_{max} - M_c)\right]}, \quad M_c \le m \le M_{max} \tag{2}$$

Sochi		
$m_b < 5.0$:	$M_w = \exp(-0.60 + 0.34\,m_b) + 2.15$	(Gasperini et al., 2013)
$m_b \geq 5.0, H \geq 70\,km$:	$M_w = 0.165\,m_b^2 - 0.372\,m_b + 2.816$	(Tsampas et al., 2016)
$H < 70\,km$:	$M_w = 1.64\,m_b - 3.18$	(Das et al., 2011)
$H < 70\,km, M_s \in [3.0\,,6.1]$:	$M_w = 0.67\,M_s + 2.12$	(Das et al., 2011)
$M_s \in [6.2\,,8.4]$:	$M_w = 1.06\,M_s - 0.38$	(Das et al., 2011)
$H \geq 70\,km, M_s \in [3.3\,,4.3]$:	$M_w = 0.67\,M_s + 2.33$	(Das et al., 2011)
$M_s \in [4.4\,,7.7]$:	$M_w = -0.006\,M_s^2 + 0.850\,M_s + 1.540$	(Tsampas et al., 2016)
Kamchatka		
$m_b < 4.5$:	$M_w = \exp(-4.37 + 0.83\,m_b) + 4.46$	(Gasperini et al., 2013)
$m_b \in [4.5\,,6.3]$:	Interpolation	(Gusev, 1991)
$M_s < 3.9, H \geq 70\,km$:	$M_w = 0.67\,M_s + 2.33$	(Das et al., 2011)
$H < 70\,km$:	$M_w = 0.67\,M_s + 2.12$	(Das et al., 2011)
$M_s \geq 3.9$:	Interpolation	(Gusev, 1991)

Table 1: Applied magnitude conversions

where $\beta = b\ln(10)$, and M_{max} is a magnitude of the strongest possible earthquake in the area.

The uncertainty of parameter β can be handled by applying the compound (Bayesian) distribution (DeGroot, 1970; Hamada et al., 2008; Klugman et al., 2008). In general, if the random variable M has a

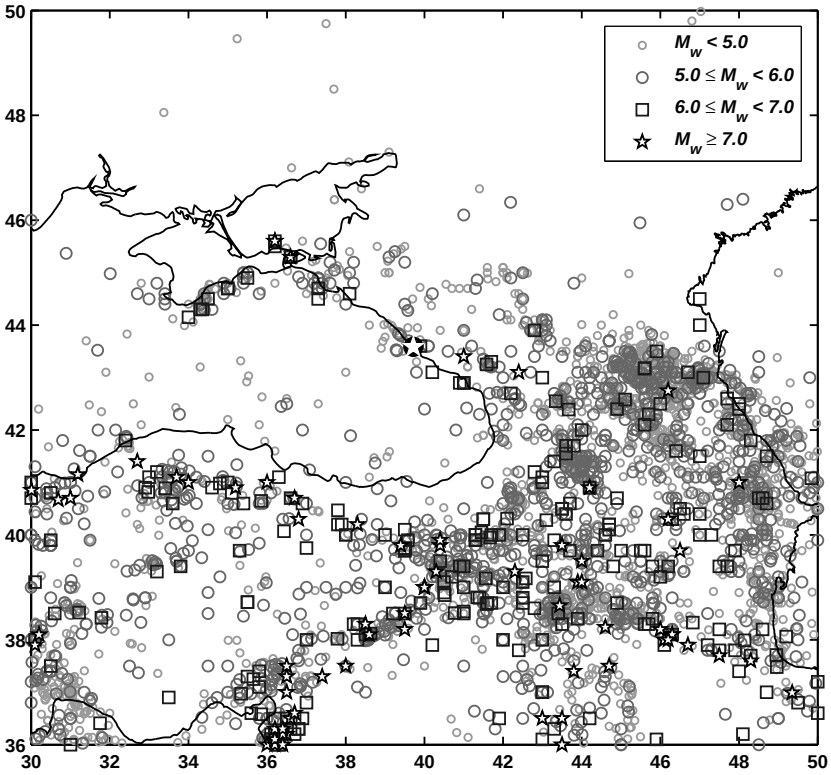

Fig. 1: Location of epicentres in the area surrounding Sochi.

CDF $F_M(m,\theta)$, with vector of parameters θ, and $f_\theta(\theta)$ denotes the probability density function (PDF) of θ, the compound CDF would be calculated as follows:

$$F_M(m) = \int_{\Omega_\theta} F_M(m,\theta)\, f_\theta(\theta)\, d\theta \tag{3}$$

Assuming that the variation of β can be modelled by a gamma distribution, the following compound CDF can be obtained (Campbell, 1982; Kijko and Graham, 1998; Kijko et al., 2016):

$$F_M(m) = C_\beta \left[1 - \left(\frac{p}{p+m-M_c}\right)^q\right], \quad M_c \le m \le M_{max} \tag{4}$$

where $p = \frac{\bar{\beta}}{\sigma^2_{\bar{\beta}}}$, $q = \left(\frac{\bar{\beta}}{\sigma_\beta}\right)^2$, $\bar{\beta}$ is the mean value of β and σ_β is its standard deviation, and C_β is a normalising constant given by:

$$C_\beta = \left[1 - \left(\frac{p}{p+M_{max}-M_c}\right)^q\right]^{-1} \tag{5}$$

The corresponding compound PDF is expressed as:

$$f_M(m) = \bar{\beta} C_\beta \left(\frac{p}{p+m-M_c}\right)^{q+1}, \quad M_c \le m \le M_{max} \tag{6}$$

Thereby, the set of required parameters for each seismic source consists of Λ, β, and M_{max}. These parameters were estimated in the following manner. First, M_{max} was estimated based on a few largest observed magnitudes (Kijko and Singh, 2011):

$$\hat{M}_{max} = M^{obs}_{max} + \frac{1}{n_0}\left(M^{obs}_{max} - \frac{1}{n_0 - 1}\sum_{i=2}^{n_0} M_{n-i+1}\right) \tag{7}$$

where M^{obs}_{max} is the largest observed earthquake magnitude, $n_0 = 10$, and M_{n-i+1} is the $(n-i)$-th largest observation.

Second, Λ and β were estimated by maximising the joint likelihood function, as described by Kijko and Sellevoll (1989; 1992). This procedure allows using the information from the whole seismic catalogue (i.e. pre-instrumental data and complete data), and accounting for uncertainties associated with the FMD and magnitude determination.

2.3 Hazard calculations

The seismic hazard at a particular site is characterised by the ground motion that has a specified probability to be exceeded at least once during the specified period of time. The assumption that the occurrence of earthquakes conforms to a stationary Poisson process allows the calculation of the probability that ground motion parameter y would exceed the value a_0 at the site at least once during time interval T:

$$P[y \ge a_0, T] = 1 - e^{-\lambda(a_0)T} \tag{8}$$

where $\lambda(a_0)$ is the annual rate of exceedance of ground motion level a_0 at the site.

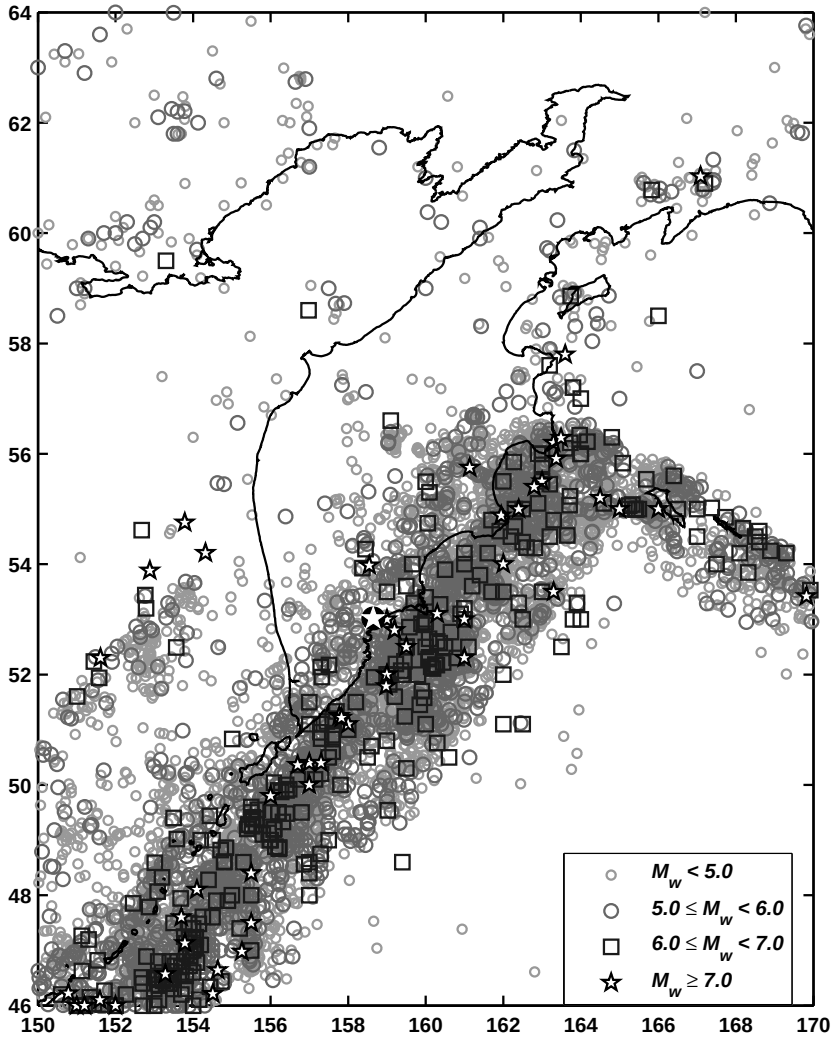

Fig. 2: Location of epicentres at the Kamchatka Peninsula

The estimation procedure for the exceedance rate $\lambda(a_0)$ depends on the applied PSHA methodology. For the Cornell-McGuire method, this value is estimated by using the following equation, based on the total probability theorem:

$$\lambda(a_0) = \sum_{i}^{N} \Lambda_i \int\int_{R\,M} P[y \geq a_0 | m, r] f_{M_i}(m) f_{R_i}(r)\, dr\, dm \tag{9}$$

where the summation is taken over all seismic sources capable of inducing significant ground motion at the site, $f_{R_i}(r)$ is the PDF of distance R, $f_{M_i}(m)$ is the PDF of magnitude M given in Eq. (6), $M_{\min}$ is the smallest magnitude considered in the analysis (in this study, $M_{\min} = 4.0$), the conditional probability of exceedance $P[y \geq a_0 | m, r]$ reflects the inherent variability of ground motion y for given magnitude m and distance r, usually calculated by using the normal (Gaussian) distribution.

In this study, as the seismic sources are modelled as a regular grid of point sources, Eq. (9) reduces to the following:

$$\lambda(a_0) = \sum_{i}^{N} \Lambda_i \int_{M_{\min}}^{M^i_{\max}} P[y \geq a_0 | m, r] f_{M_i}(m) dm \tag{10}$$

By increasing the value a_0 and repeating these calculations, the seismic hazard curve is constructed.

The Parametric-Historic method is oriented more empirically. Only the sources that induce ground motions y in excess of a fixed lower threshold $a_{\min}$ are taken into account. The magnitude range is subdivided into small intervals Δm and for each source the cumulative rate of exceedance is calculated by summing the incremental rates. The total annual rate of exceedance $\lambda(a_0)$ is calculated by summation over all contributing sources:

$$\lambda(a_0) = P[y \geq a_0] \sum_{i}^{N_s} \sum_{j}^{N_m} \Lambda_i (a \geq a_{\min}) \int_{m_j - \Delta m/2}^{m_j + \Delta m/2} f_{M_i}(m)\, dm \tag{11}$$

where N_s is the number of seismic sources that induce ground motions y in excess of the fixed lower threshold $a_{\min}$, N_m is the number of intervals Δm between $M_{\min}$ and $M^i_{\max}$, and $P[y \geq a_0]$ is the probability of exceedance, estimated from the empirical distribution of y at a site of interest.

The third considered PSHA procedure is based on a synthetic catalogue of seismic events. The synthetic catalogue is generated by the Monte Carlo simulation technique, based on the estimated seismic parameters Λ, β, and $M_{\max}$. The duration of the synthetic catalogue T_c should be sufficient to allow for reliable hazard estimation. In this study, two probability levels are considered, namely, 10% and 2% probabilities of exceedance in 50 years, which correspond to return periods of approximately 475 and 2475 years, respectively. In this study, the duration of the synthetic catalogues was equal to a hundred times the return period.

The estimation of the annual rate of exceedance $\lambda(a_0)$ from the synthetic catalogue is straightforward. The ground motion parameter y is calculated for each event of the synthetic catalogue and a cumulative histogram of y is calculated. Subsequently, the cumulative histogram is normalised by the timespan of the synthetic catalogue T_c, and the required annual rate of exceedance $\lambda(a_0)$ is obtained from the normalised histogram.

2.4 Selection of the GMPEs

Estimates of the expected ground motion at the site of interest are fundamental factors in seismic hazard analysis. The ground motion is characterised by a particular parameter, usually a horizontal peak ground acceleration (PGA), peak ground velocity, or spectral acceleration. GMPEs are employed to estimate ground motion parameters for use in both the deterministic and the probabilistic seismic hazard analyses. These equations allow estimation of the median values of the ground motion parameters, based on the earthquake magnitude, source to site distance, local soil conditions, fault mechanism, and other parameters. The GMPEs are usually empirical equations obtained by means of regression analysis (e.g. Joyner and Boore, 1993). A large variety of GMPEs for different parts of the world have been developed over the years (Douglas, 2011).

As regards the regions selected for analysis, despite continuous studies of the characteristics of the strong ground motions at the North Caucasus (Pavlenko, 2008; 2009; 2016; Pavlenko and Pavlenko, 2016) and at the Kamchatka Peninsula (Gusev et al., 1997; Petukhin et al., 1999; Chubarova et al., 2010), regional GMPEs have not been developed yet. In such instances, a common practice is to adopt the

Reference	Scaling parameters	Sochi	Kamchatka	Weight
Akkar and Bommer (2007)	M_w, R_{JB}	✓	✓	0.2
Boore and Atkinson (2008)	M_w, R_{JB}	✓	✓	0.2
Campbell and Bozorgnia (2008)	M_w, R_{rup}	✓	✓	0.2
Cauzzi and Faccioli (2008)	M_w, R_{hyp}	✓	✓	0.2
Chiou and Youngs (2008)	M_w, R_{rup}	✓	✓	0.2
Youngs et al. (1997)	M_w, R_{rup}	–	✓	0.34
Atkinson and Boore (2003)	M_w, R_{rup}	–	✓	0.33
Kanno et al. (2006)	M_w, R_{rup}	–	✓	0.33

Table 2: The GMPEs recommended by the GEM

GMPEs developed for other regions with similar tectonic properties (e.g. Stafford et al., 2008; Delavaud et al., 2009). Since the purpose of the current study is to compare the different methods of PSHA rather than to assess the seismic hazard itself, the adoption of particular GMPEs should not affect the results radically. Therefore, in this study, a set of GMPEs recommended by the Global Earthquake Model (GEM, http://www.globalquakemodel.org) project is used. These GMPEs are listed in Table 2.

The GMPEs of Akkar and Bommer (2007) and Cauzzi and Faccioli (2008) have been developed for implementation in the European region. Akkar and Bommer (2007) used strong motion data from Europe and the Middle East for their study, while Cauzzi and Faccioli (2008) compiled the database by including the strong motion records from Japan, Iran, California, Turkey, Iceland, and Italy. The GMPEs of Boore and Atkinson (2008), Campbell and Bozorgnia (2008), and Chiou and Youngs (2008) have been developed as contributions to the Next Generation Attenuation project of the Pacific Earthquake Engineering Research Center (peer.berkeley.edu), and are considered globally applicable to shallow crustal earthquakes in active tectonic regions.

Youngs et al. (1997) and Atkinson and Boore (2003) have developed globally applicable GMPEs for subduction zone earthquakes, based on the global strong motion databases, whereas, the GMPE of Kanno et al. (2006) has been developed by using the data from Japan, California, and Turkey. Youngs et al. (1997) and Atkinson and Boore (2003) categorised earthquakes as interface events (shallow-angle thrust events that occur on the interface between the subducting and the overriding plates, usually not deeper than 50 km) and intraslab events (events that occur within the subducting oceanic plate and which are typically high-angle normal faulting events). Kanno et al. (2006) distinguished between shallow and deep earthquakes.

The seismic hazard in Sochi and the surrounding region is partially attributable to the proximity of the area to the Caucasus Mountains, a part of the Iran-Caucasus-Anatolia seismic region, characterised by high seismic activity. Furthermore, numerous strong and moderate earthquakes have been reported in the Sochi area and in other parts of the Black Sea coastal area, as well as in the Black Sea itself.

In comparison with the seismicity of the Sochi region, that of the Kamchatka Peninsula represents a greater challenge. The seismicity of the Kamchatka Peninsula is characterised by subduction earthquakes on the south eastern coast, where seismicity is dominated by the events occurring at the Kuril-Kamchatka Trench. At the north end of the peninsula, seismicity is characterised by less frequent crustal earthquakes. To the west of the peninsula, in the Sea of Okhotsk, several large deep-focus earthquakes have occurred in recent times, including the great M_w 8.3 earthquake of May 24, 2013 (Chebrova et al., 2015).

Along the south eastern coast, in area that extends deep into the peninsula, the ground motions could be caused by either the subduction earthquakes occurring on the dipping Pacific Plate beneath the peninsula, or by the crustal earthquakes. This area was modelled as a transition zone of mixed seismicity, where both types of earthquakes contribute to strong ground motions. The structure of the Kamchatka subduction zone was explored in detail by Gorbatov et al. (1997). The ground motions in the transition

zone were estimated as the weighted average of the outputs of two GMPEs, one developed for crustal seismicity, and the second developed for subduction earthquakes:

$$\begin{cases} y = p_c y_c + p_s y_s \\ \sigma = \sqrt{p_c^2 \sigma_c^2 + p_s^2 \sigma_s^2} \end{cases} \quad (12)$$

where p represent normalised weights that reflect the relative probability for ground motion to be induced by a subduction or crustal event, y is the median ground motion value, and σ is the corresponding standard deviation, subscripts c and s mean crustal and subduction.

Epistemic uncertainty was handled by using the logic tree formalism (e.g. Bommer et al., 2005), and a set of alternative hazard curves was calculated by using the GMPEs, from which the mean hazard curve was selected to characterise seismic hazard. The weights of the set of GMPEs are listed in Table 2.

3 Results and discussion

Figures 3 and 4 show the seismic hazard maps for PGA for the two considered areas. In these figures, the hazard maps for exceedance probability of 10% in 50 years (return period of 475 years) are shown in the upper row; whereas, in the lower row, the maps are shown for exceedance probability of 2% in 50 years (return period of 2475 years). In the computation of seismic hazard, the grid size was set to 0.1°for the Sochi area and to 0.2°for the Kamchatka area.

The shape of the hazard contours reflects the observed regional seismicity, with the higher hazard being concentrated near the epicentres of the major seismic events. When the return period is increased from 475 years to 2475 years, the seismic hazard estimates increase by a factor of nearly 1.9, while the shape of the contours remains unchanged.

It could be interesting to subject these maps to a test to indicate which of the methods provides the most realistic result. Objective testing of the PSHA results is a significant problem, which has been discussed by many authors (e.g. McGuire, 1979; Ward, 1995; Ordaz and Reyes, 1999; Beauval et al., 2008; Stirling and Gerstenberger, 2010; Stein et al., 2011; Kossobokov and Nekrasova, 2012; Stirling, 2012; Wyss et al., 2012; Stein et al., 2012; Iervolino, 2013; Mezcua et al., 2013; Stein et al., 2015; Sokolov and Ismail-Zadeh, 2016), with various approaches being proposed.

There are two main categories of tests, of which the first relates to testing the modelled rate of exceedance against the observed number of ground motion exceedances (e.g. Ordaz and Reyes, 1999; Stirling and Gerstenberger, 2010; Mezcua et al., 2013). The second category of tests relies on comparison between the modelled and the observed levels of ground motion (e.g. Ward, 1995; Miyazawa and Mori, 2009; Kossobokov and Nekrasova, 2012).

However, the question of the adequacy of the PSHA methods is beyond the scope of the current study.

Moreover, the testing of seismic hazard estimates is a relatively new and debatable aspect of PSHA (e.g. Stein et al., 2011; Hanks et al., 2012; Stirling, 2012), and no consensus has been reached on how such testing should be performed. Consequently, the current analysis is restricted to a quantitative comparison of the obtained PSHA maps.

The hazard estimates were compared at the sites along two profiles, passing through the highest, moderate, and the lowest hazard areas of the maps, as shown in Figs. 3 and 4. Figures 5 and 6 show the levels of PGA along these profiles. The trends observed along both profiles are similar, namely, the Cornell-McGuire method yields the highest hazard estimates; whereas, those obtained with the Parametric-Historic method and the method based on the Monte Carlo technique are slightly lower. The ratios of the PGA estimates along the two profiles were calculated for more explicit comparison (Table 3).

The relative difference between the PGA estimates along profile 1 slightly increases with the increasing return period. On average, the relative difference between the PGA estimates based on the Parametric-Historic and the Cornell-McGuire methods is about 5% for both return periods; whereas, that of the

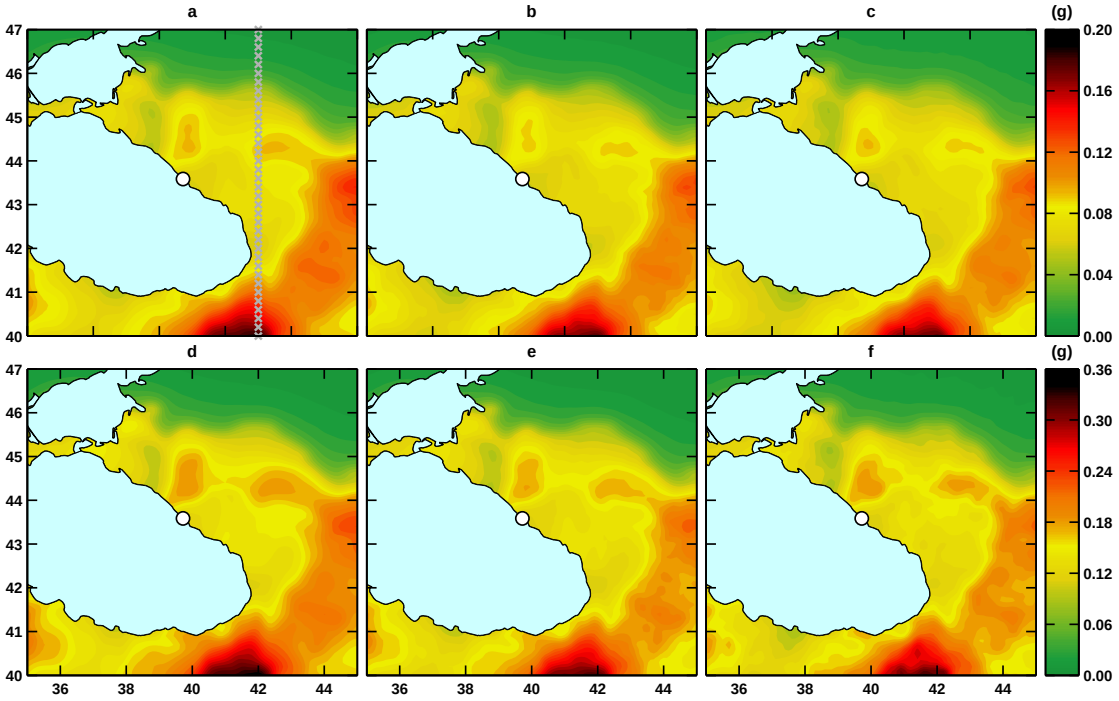

Fig. 3: Comparison of seismic hazard maps for Sochi and surrounding area. Left to right: the Cornell-McGuire method, the Parametric-Historic method, and the method based on the Monte Carlo technique. Upper row: T_R = 475 years, lower row: T_R = 2475 years. White circle shows location of Sochi. Profile 1 is shown by grey crosses in Fig. 3a

	Profile 1				Profile 2			
T_R = 475 years	$A_{\max}(g)$	$R_{\max}$	$< R >$	$R_{\min}$	$A_{\max}(g)$	$R_{\max}$	$< R >$	$R_{\min}$
Cornell-McGuire	0.188				0.472			
Parametric-Historic	0.180	0.955	0.952	0.935	0.423	0.896	0.919	0.940
Monte Carlo	0.178	0.944	0.943	0.935	0.411	0.871	0.900	0.919
T_R = 2475 years								
Cornell-McGuire	0.352				0.894			
Parametric-Historic	0.329	0.934	0.948	0.921	0.797	0.891	0.919	0.943
Monte Carlo	0.320	0.910	0.937	0.920	0.780	0.872	0.902	0.924

$A_{\max}$ - maximum PGA estimate, $R_{\max} = (A_{\max}/A^{CM}_{\max})$, $< R >=< (A/A^{CM}) >$, $R_{\min} = (A_{\min}/A^{CM}_{\min})$
A^{CM} - estimates of the Cornell-McGuire method, A - estimates of the two other methods

Table 3: Comparison of seismic hazard estimates along two profiles

method based on the Monte Carlo technique on average 6% below the estimates of the Cornell-McGuire method for both return periods.

Along profile 2, the relative difference between the PGA estimates decreases slightly as the hazard level decreases (Table 3), and the ratios are similar for both return periods. The PGA estimates of the Parametric-Historic method are on average 8% below the estimates of the Cornell-McGuire method; whereas, those of the method based on the Monte Carlo technique are on average 10% below the estimates of the Cornell-McGuire method.

Judging by the averaged values of the ratios, the variation among the results based on the three methods is relatively low, but has a systematic nature.

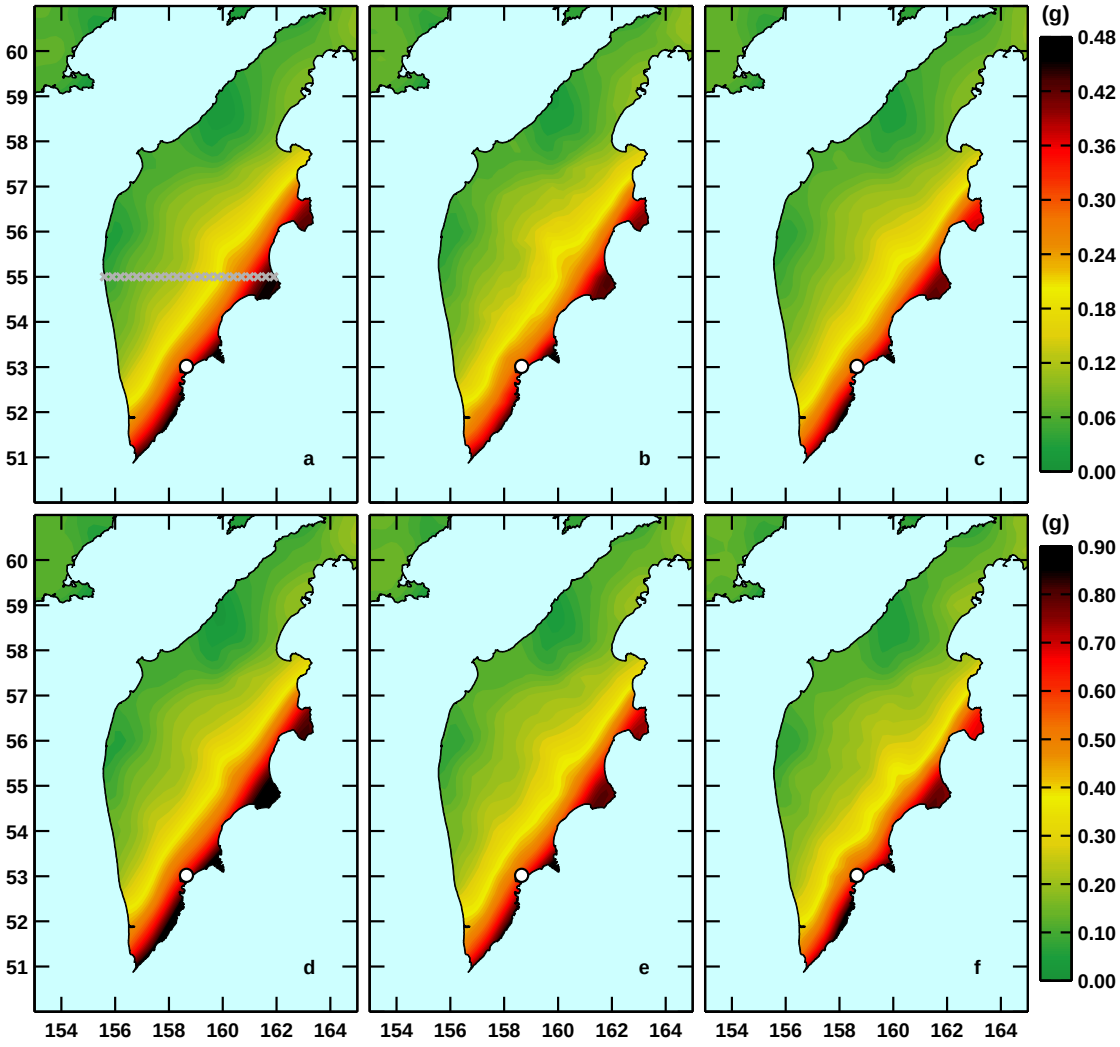

Fig. 4: Comparison of seismic hazard maps for Kamchatka. Left to right: the Cornell-McGuire method, the Parametric-Historic method, and the method based on the Monte Carlo technique. Upper row: T_R = 475 years, lower row: T_R = 2475 years. White circle shows location of Petropavlovsk-Kamchatskiy. Profile 2 is shown by grey crosses in Fig. 4a

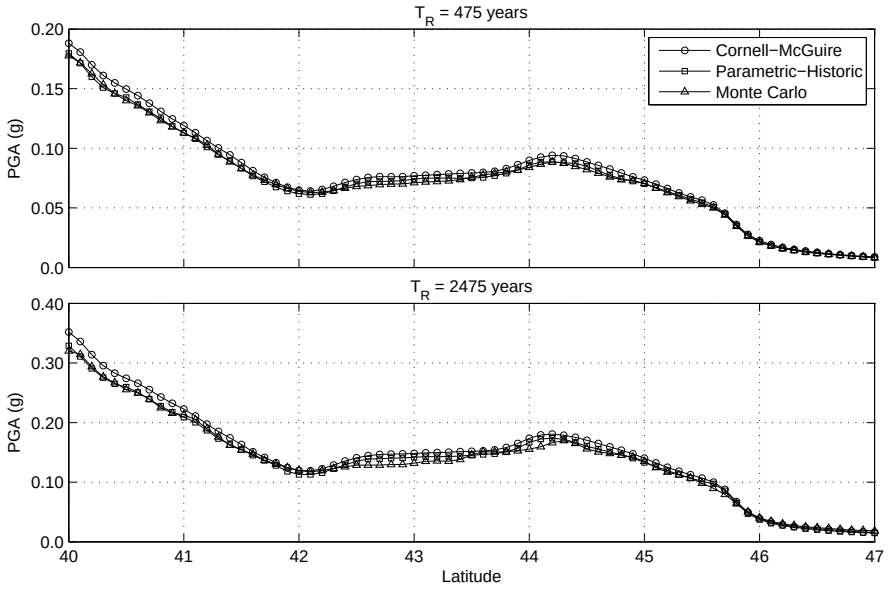

Fig. 5: Hazard levels along profile 1

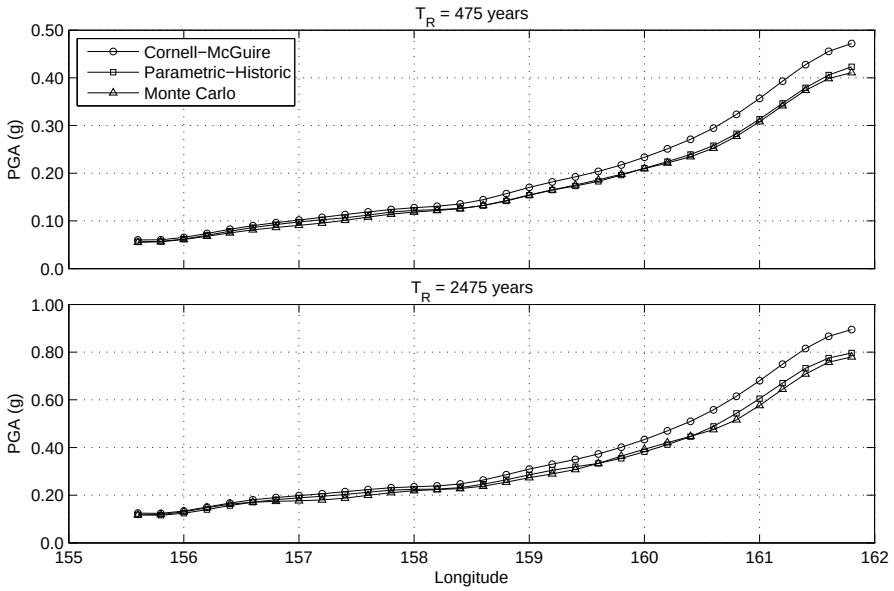

Fig. 6: Hazard levels along profile 2

4 Conclusion

In this study, seismic hazard estimates obtained by using three different PSHA methods were compared. For the purposes of comparison all uncertainties in parameters of seismicity were removed and a single long-term synthetic catalogue was generated and used in the calculations. For comparison, the seismic hazard maps were prepared for two regions of Russia, and the PGA estimates were compared for return periods of 475 and 2475 years. The results indicated that the choice of a particular method for conducting PSHA has relatively little effect on the hazard estimates when the same seismic source model was used in the calculations. The comparison indicated that the Cornell-McGuire method systematically yielded the highest estimates of PGA, whereas the Parametric-Historic method and the method based on the Monte Carlo technique produced similar results, which were slightly below that of the Cornell-McGuire method. The analysis for the two regions considered indicated that the relative difference between the results of the three methods was systematic, remaining virtually unchanged when the return period increased from 475 to 2475 years. For the Sochi region, characterised by high seismic activity, this difference was within 6%; whereas, for the Kamchatka region, where seismic activity is very high, the difference was up to 10%. These results suggest that for regions of moderate seismic activity, all three methods would provide closely related seismic hazard estimates. However, difference among the results would apparently become more pronounced for regions characterised by high seismic activity.

Acknowledgements We are grateful to Dr. Nina Medvedeva from the Schmidt Institute of Physics of the Earth of the Russian Academy of Sciences for provided earthquake catalogue, and to the USGS for their data (available at http://earthquake.usgs.gov). We are grateful to two anonymous reviewers for their valuable comments and suggestions.

References

Akkar S, Bommer JJ (2007) Prediction of elastic displacement response spectra in Europe and the Middle East. Earthq Eng Struct Dyn 36:1275–1301, doi: 10.1002/eqe.679

Amorèse D (2007) Applying a change-point detection method on frequency-magnitude distributions. Bull Seismol Soc Am 97(5):1742–1749, doi: 10.1785/0120060181

Assatourians K, Atkinson GM (2013) EqHaz: an open-source probabilistic seismic-hazard code based on the Monte Carlo simulation approach. Seismol Res Lett 84(3):516–524, doi: 10.1785/0220120102

Atkinson GM, Boore DM (2003) Empirical ground-motion relations for subduction-zone earthquakes and their application to Cascadia and other regions. Bull Seismol Soc Am 93(4):1703–1729, doi: 10.1785/0120020156

Beauval C, Scotti O, Bonilla F (2006) The role of seismicity models in probabilistic seismic hazard estimation: comparison of a zoning and a smoothing approach. Geophys J Int 165(2):584–595, doi: 10.1111/j.1365-246X.2006.02945.x

Beauval C, Bard PY, Hainzl S, Guéguen P (2008) Can strong-motion observations be used to constrain probabilistic seismic-hazard estimates? Bull Seismol Soc Am 98(2):509–520, doi: 10.1785/0120070006

Bommer JJ, Scherbaum F, Bungum H, Cotton F, Sabetta F, Abrahamson NA (2005) On the use of logic trees for ground-motion prediction equations in seismic-hazard analysis. Bull Seismol Soc Am 95(2):377–389, doi: 10.1785/0120040073

Boore DM, Atkinson GM (2008) Ground-motion prediction equations for the average horizontal component of PGA, PGV, and 5%-damped PSA at spectral periods between 0.01 s and 10.0 s. Earthq Spectra 24(1):99–138, doi: 10.1193/1.2830434

Budnitz RJ, Apostolakis G, Boore DM, Cluff LS, Coppersmith KJ, Cornell CA, Morris PA (1997) Recommendations for probabilistic seismic hazard analysis: guidance on uncertainty and use of experts. U.S. Nuclear Regulatory Commission Report NUREG/CR-6372

Campbell KW (1982) Bayesian analysis of extreme earthquake occurrences. Part I. Probabilistic hazard model. Bull Seismol Soc Am 72(5):1689–1705

Campbell KW, Bozorgnia Y (2008) NGA ground motion model for the geometric mean horizontal component of PGA, PGV, PGD and 5% damped linear elastic response spectra for periods ranging from 0.01 to 10 s. Earthq Spectra 24(1):139–171, doi: 10.1193/1.2857546

Cauzzi C, Faccioli E (2008) Broadband (0.05 to 20 s) prediction of displacement response spectra based on worldwide digital records. J Seismol 12:453–475, doi: 10.1007/s10950-008-9098-y

Chebrova AY, Chebrov VN, Gusev AA, Lander AV, Guseva EM, Mityushkina SV, Raevskaya AA (2015) The impacts of the M_W 8.3 Sea of Okhotsk earthquake of May 24, 2013 in Kamchatka and worldwide. J Volcanol Seismol 9(4):223–241, doi: 10.1134/S074204631504003X

Chiou BSJ, Youngs RR (2008) An NGA model for the average horizontal component of peak ground motion and response spectra. Earthq Spectra 24(1):173–215, doi: 10.1193/1.2894832
Chubarova OS, Gusev AA, Chebrov VN (2010) The ground motion excited by the Olyutorskii earthquake of April 20, 2006 and by its aftershocks based on digital recordings. J Volcanol Seismol 4(2):126–138, doi: 10.1134/S0742046310020065
Cornell CA (1968) Engineering seismic risk analysis. Bull Seismol Soc Am 58(5):1583–1606
Das R, Wason HR, Sharma ML (2011) Global regression relations for conversion of surface wave and body wave magnitudes to moment magnitude. Nat Hazards 59(2):801–810, doi: 10.1007/s11069-011-9796-6
DeGroot MH (1970) Optimal Statistical Decisions. McGraw-Hill, New York
Delavaud E, Scherbaum F, Kuehn N, C R (2009) Information-theoretic selection of ground-motion prediction equations for seismic hazard analysis: an applicability study using Californian data. Bull Seismol Soc Am 99(6):3248–3263, doi: 10.1785/0120090055
Douglas J (2011) Ground-motion prediction equations 1964-2010. Final Rept. RP-59356-FR, Bureau de Recherches Géologiques et Minières (BRGM), Orléans, France, 444 pp. Available at http://peer.berkeley.edu
Ebel JE, Kafka AL (1999) A Monte Carlo approach to seismic hazard analysis. Bull Seismol Soc Am 89(4):854–866
Frankel A (1995) Mapping seismic hazard in the Central and Eastern United States. Seismol Res Lett 66(4):8–21, doi: 10.1785/gssrl.66.4.8
Frankel AD, Petersen MD, Mueller CS, Haller KM, Wheeler RL, Leyendecker EV, Wesson RL, Harmsen SC, Cramer CH, Perkins DM, Rukstales KS (2002) Documentation for the 2002 update of the national seismic hazard maps. U.S. Geological Survey, Open-File Report 02-420
Gardner JK, Knopoff L (1974) Is the sequence of earthquakes in Southern California, with aftershocks removed, Poissonian? Bull Seismol Soc Am 64(5):1363–1367
Gasperini P, Lolli B, Vannucci G (2013) Body-wave magnitude m_b is a good proxy of moment magnitude M_w for small earthquakes ($m_b < 4.5 - 5.0$). Seismol Res Lett 84(6):932–937, doi: 10.1785/0220130105
Goda K, Aspinall W, Taylor CA (2013) Seismic hazard analysis for the U.K.: sensitivity to spatial seismicity modelling and ground motion prediction equations. Seismol Res Lett 84(1):112–129, doi: 10.1785/0220120064
Gorbatov A, Kostoglodov V, Suárez G, Gordeev E (1997) Seismicity and structure of the Kamchatka subduction zone. J Geophys Res 102(B8):17,883–17,898, doi: 10.1029/96JB03491
Gusev AA (1991) Intermagnitude relationships and asperity statistics. Pure Appl Geophys 136(4):515–527, doi: 10.1007/BF00878585
Gusev AA, Gordeev EI, Guseva EM, Petukhin AG, Chebrov VN (1997) The first version of the $A_{max}(M_W, R)$ relationship for Kamchatka. Pure Appl Geophys 149(2):299–312, doi: 10.1007/s000240050027
Gutenberg B, Richter CF (1944) Frequency of earthquakes in California. Bull Seismol Soc Am 34(4):185–188
Hamada MS, Wilson AG, Reese CS, Martz HF (2008) Bayesian Reliability. Springer, New York
Hanks TC, Beroza GC, Toda S (2012) Have recent earthquakes exposed flaws in or misunderstandings of probabilistic seismic hazard analysis? Seismol Res Lett 83(5):759–564, doi: 10.1785/0220120043
Hong HP, Goda K, Davenport AG (2006) Seismic hazard analysis: a comparative study. Can J Civ Eng 33(9):1156–1171, doi: 10.1139/l06-062
Iervolino I (2013) Probabilities and fallacies: why hazard maps cannot be validated by individual earthquakes. Earthq Spectra 29(3):1125–1136, doi: 10.1193/1.4000152
Joyner WB, Boore DM (1993) Methods of regression analysis of strong motion data. Bull Seismol Soc Am 83(2):469–487
Kanno T, Narita A, Morikawa N, Fujiwara H, Fukushima Y (2006) A new attenuation relation for strong ground motion in Japan based on recorded data. Bull Seismol Soc Am 96(3):879–897, doi: 10.1785/0120050138
Kijko A, Graham G (1998) Parametric-historic procedure for probabilistic seismic hazard analysis. Part I: Estimation of maximum regional magnitude m_{max}. Pure Appl Geophys 152(3):413–442, doi: 10.1007/s000240050161
Kijko A, Graham G (1999) "Parametric-historic" procedure for probabilistic seismic hazard analysis. Part II: Assessment of seismic hazard at specified site. Pure Appl Geophys 154(1):1–22, doi: 10.1007/s000240050218
Kijko A, Sellevoll MA (1989) Estimation of earthquake hazard parameters from incomplete data files. Part I. Utilization of extreme and complete catalogs with different threshold magnitudes. Bull Seismol Soc Am 79(3):645–654
Kijko A, Sellevoll MA (1992) Estimation of earthquake hazard parameters from incomplete data files. Part II. Incorporation of magnitude heterogeneity. Bull Seismol Soc Am 82(1):120–134
Kijko A, Singh M (2011) Statistical tools for maximum possible earthquake magnitude estimation. Acta Geophys Pol 59(4):674–700, doi: 10.2478/s11600-011-0012-6
Kijko A, Smit A, Sellevoll MA (2016) Estimation of earthquake hazard parameters from incomplete data files. Part III. Incorporation of uncertainty of earthquake-occurrence model. Bull Seismol Soc Am 106(3):1210–1222, doi: 10.1785/0120150252
Klugman SA, Panjer HH, Willmot GE (2008) Loss Models: From Data to Decisions. John Wiley & Sons, Inc., Hoboken, New Jersey
Kossobokov VG, Nekrasova AK (2012) Global seismic hazard assessment program maps are erroneous. Seism Instrum 48(2):162–170, doi: 10.3103/S0747923912020065
McGuire RK (1976) Fortran program for seismic risk analysis. U.S. Geological Survey, Open-File Report 76-67
McGuire RK (1978) FRISK: computer program for seismic risk analysis using faults as earthquake sources. U.S. Geological Survey, Open-File Report 78-1007

McGuire RK (1979) Adequacy of simple probability models for calculating felt-shaking hazard, using the Chinese earthquake catalog. Bull Seismol Soc Am 69(3):877–892
McGuire RK (1993) Computations of seismic hazard. Ann Geofisc 36(3-4):181–200, doi: 10.4401/ag-4263
Mezcua J, Rueda J, García Blanco RM (2013) Observed and calculated intensities as a test of a probabilistic seismic-hazard analysis of Spain. Seismol Res Lett 84(5):772–780, doi: 10.1785/0220130020
Milne WG, Davenport AG (1969) Distribution of earthquake risk in Canada. Bull Seismol Soc Am 59(2):729–754
Miyazawa M, Mori J (2009) Test of seismic hazard map from 500 years of recorded intensity data in Japan. Bull Seismol Soc Am 99(6):3140–3149, doi: 10.1785/0120080262
Molina S, Lindholm CD, Bungum H (2001) Probabilistic seismic hazard analysis: zoning free versus zoning methodology. Bollettino di Geofisica Teorica ed Applicata 42(1-2):19–39
Musson RMW (2000) The use of Monte Carlo simulations for seismic hazard assessment in the U.K. Ann Geofisc 43(1):1–9, doi: 10.4401/ag-3617
Ordaz M, Reyes C (1999) Earthquake hazard in Mexico City: observations versus computations. Bull Seismol Soc Am 89(5):1379–1383
Pavlenko OV (2008) Characteristics of seismic wave attenuation in the crust and upper mantle of the Northern Caucasus. Izv, Phys Solid Earth 44(6):487–494, doi: 10.1134/S1069351308060049
Pavlenko OV (2009) The study of the radiation characteristics and propagation of seismic waves in the North Caucasus by modeling the accelerograms of the recorded earthquakes. Izv, Phys Solid Earth 45(10):874–884, doi: 10.1134/S106935130910005X
Pavlenko OV (2011) Regional differences in the characteristics of seismic wave emission and propagation in Kamchatka and the Northern Caucasus. Doklady Earth Sciences 438(2):846–852, doi: 10.1134/S1028334X11060225
Pavlenko OV (2016) The Q-factor estimates for the crust and upper mantle in the vicinity of Sochi and Anapa (North Caucasus). Izv, Phys Solid Earth 52(3):353–363, doi: 10.1134/S1069351316030101
Pavlenko VA, Pavlenko OV (2016) The seismic wave absorption in the crust and upper mantle in the vicinity of the Kislovodsk seismic station. Izv, Phys Solid Earth 52(4):492–502, doi: 10.1134/S1069351316030113
Petersen MD, Moschetti MP, Powers PM, Mueller CS, Haller KM, Frankel AD, Zeng Y, Rezaeian S, Harmsen SC, Boyd OS, Field N, Chen R, Rukstales KS, Luco N, Wheeler RL, Williams RA, Olsen AH (2014) Documentation for the 2014 update of the United States National seismic hazard maps. U.S. Geological Survey, Open-File Report 2014-1091, doi: 10.3133/ofr20141091
Petukhin AG, Gusev AA, Guseva EM, Gordeev EI, Chebrov VN (1999) Preliminary model for scaling of Fourier spectra of strong ground motion recorded on Kamchatka. Pure Appl Geophys 156(3):445–468, doi: 10.1007/s000240050307
Shumilina LS, Gusev AA, Pavlov VM (2000) An improved technique for determination of seismic hazard. J Earthq Predict Res 8:104–110
Sokolov V, Ismail-Zadeh A (2016) On the use of multiple-site estimations in probabilistic seismic-hazard assessment. Bull Seismol Soc Am 106(5):2233–2243, doi: 10.1785/0120150306
Spada M, Wiemer S, Kissling E (2011) Quantifying a potential bias in probabilistic seismic hazard assessment: seismotectonic zonation with fractal properties. Bull Seismol Soc Am 101(6):2694–2711, doi: 10.1785/0120110006
Stafford PJ, Strasser FO, Bommer JJ (2008) An evaluation of the applicability of the NGA models to ground-motion prediction in the Euro-Mediterranean region. Bull Earthquake Eng 6(2):149–177, doi: 10.1007/s10518-007-9053-2
Stein S, Geller R, Liu M (2011) Bad assumptions or bad luck: why earthquake hazard maps need objective testing. Seismol Res Lett 82(5):623–626, doi: 10.1785/gssrl.82.5.623
Stein S, Geller R, Liu M (2012) Why earthquake hazard maps often fail and what to do about it. Tectonophysics 562-563:1–25, doi: 10.1016/j.tecto.2012.06.047
Stein S, Spencer BD, Brooks EM (2015) Metrics for assessing earthquake-hazard map performance. Bull Seismol Soc Am 105(4):2160–2173, doi: 10.1785/0120140164
Stirling M (2012) Earthquake hazard maps and objective testing: the hazard mapper's point of view. Seismol Res Lett 83(2):231–232, doi: 10.1785/gssrl.83.2.231
Stirling M, Gerstenberger M (2010) Ground motion-based testing of seismic hazard models in New Zealand. Bull Seismol Soc Am 100(4):1407–1414, doi: 10.1785/0120090336
Tsampas AD, Scordilis EM, Papazachos CB, Karakaisis GF (2016) Global-magnitude scaling relations for intermediate-depth and deep-focus earthquakes. Bull Seismol Soc Am 106(2):418–434, doi: 10.1785/0120150201
Veneziano D, Cornell CA, O'hara T (1984) Historical method for seismic hazard analysis. Electric Power Research Institute, report, NP-3438, Palo Alto
Ward SN (1995) Area-based tests of long-term seismic hazard predictions. Bull Seismol Soc Am 85(5):1285–1298
Wiemer S, García-Fernández M, Burg JP (2009) Development of a seismic source model for probabilistic seismic hazard assessment of nuclear power plant sites in Switzerland: the view from PEGASOS Expert Group 4 (EG1d). Swiss J Geosci 102(1):189–209, doi: 10.1007/s00015-009-1311-7
Woo G (1996) Kernel estimation methods for seismic hazard area source modeling. Bull Seismol Soc Am 86(2):353–362
Wyss M, Nekrasova A, Kossobokov V (2012) Errors in expected human losses due to incorrect seismic hazard estimates. Nat Hazards 62(3):927–935, doi: 10.1007/s11069-012-0125-5
Yemanov AA, Yemanov AF, Kuznecov KG, Leskova YV, Novikov IS, Sychev IV, Fateev AV (2007) Seismic hazard assessment of the south territory of Kuzbass. NNC RK Bull 2(30):113–127
Youngs RR, Chiou SJ, Silva WJ, Humphrey JR (1997) Strong ground motion attenuation relationships for subduction zone earthquakes. Seismol Res Lett 68(1):58–73, doi: 10.1785/gssrl.68.1.58